

Hard X-ray Spectrographs with Resolution Beyond 100 μeV

Yuri Shvyd'ko,^{1,*} Stanislav Stoupin,¹ Kiran Mundboth,² and Jungho Kim¹

¹*Advanced Photon Source, Argonne National Laboratory, Argonne, Illinois 60439, USA*

²*Diamond Light Source Ltd, Didcot Oxfordshire OX11 0DE, UK*

Spectrographs take snapshots of photon spectra with array detectors by dispersing photons of different energies into distinct directions and spacial locations. Spectrographs require optics with a large angular dispersion rate as the key component. In visible light optics diffraction gratings are used for this purpose. In the hard x-ray regime, achieving large dispersion rates is a challenge. Here we show that multi-crystal, multi-Bragg-reflection arrangements feature cumulative angular dispersion rates almost two orders of magnitude larger than those attainable with a single Bragg reflection. As a result, the multi-crystal arrangements become potential dispersing elements of hard x-ray spectrographs. The hard x-ray spectrograph principles are demonstrated by imaging a spectrum of photons with a record high resolution of $\Delta E \simeq 90 \mu\text{eV}$ in hard x-ray regime, using multi-crystal optics as dispersing element. The spectrographs can boost research using inelastic ultra-high-resolution x-ray spectroscopies with synchrotrons and seeded XFELs.

PACS numbers: 42.25.-p, 41.50.+h, 07.85.Nc, 78.70.Ck, 07.85.Fv

A dream x-ray spectrometer is actually a spectrograph that images x-ray spectra in one shot, and with an ultimate spectral resolution. State of the art single shot x-ray spectrometers [1–4] are imaging spectra with array detectors, using Bragg's law dispersion (BD). BD links the angle of incidence θ to the energy E of photons Bragg reflected from the crystal atomic planes. However, the spectral resolution of the BD-spectrometers is always limited by the Bragg reflection (Darwin) bandwidth.

Angular dispersion (AD) is one way how to overcome the Darwin width limitation and substantially improved spectral resolution of x-ray optics [5, 6]. AD is a variation of the photon angle of reflection θ' , for a fixed incidence angle θ , with the photon energy E . AD takes place in Bragg diffraction, albeit only if the diffracting atomic planes are at a nonzero angle $\eta \neq 0$ (asymmetry angle) to the entrance crystal surface [5, 7, 8], see Fig. 1(b).

Unlike BD, AD links θ' to E for a fixed θ . AD is independent of the Darwin width, and can be therefore used to resolve much narrower spectral features. Using angular-dispersive monochromators, x-rays were already monochromatized to bandwidths (0.45 meV) almost two orders of magnitude smaller than the width of the Bragg reflections (27 meV) involved [9]. New concepts are required, however, to realize single shot angular-dispersive spectrographs.

We show here that multi-Bragg-reflection arrangements feature, in theory and in experiment, cumulative angular dispersion rates almost two orders of magnitude greater than those attainable in a single Bragg reflection. An angular-dispersive x-ray spectrograph of a Czerny-Turner-type [10] is introduced with the enhanced angular-dispersive optics as a “diffraction grating”. A record high spectral resolution of $\Delta E \simeq 90 \mu\text{eV}$ is demonstrated in the hard x-ray regime.

Czerny-Turner grating spectrographs are nowadays standard in infrared, visible, and ultraviolet spectro-

scopies [11, 12]. In its classical arrangement, the spectrographs comprise, first, a collimating mirror M_C , which collects photons from a radiation source S and collimates the photon beam - see Fig. 1(a); second, an angular-dispersive element DE such as a diffraction grating or a prism, which disperses photons of different energies into different directions; third, a curved mirror M_F which focuses photons of different energies onto different locations $x(E)$, and, last but not least, a spatially sensitive detector Det placed in the focal plane to record the whole photon spectrum. To achieve high resolution, the most important factor is the magnitude of the AD rate $\mathcal{D} = \delta\theta'/\delta E$, which measures the variation of the reflection angle θ' with photon energy E upon reflection from the dispersing element. For the given mirror focal length \mathcal{F} ($M_F \rightarrow Det$), the AD rate \mathcal{D} determines the variation of the source image position $x(E)$ on the detector with respect to photon energy: $\delta x(E) = \mathcal{D}\mathcal{F}\delta E$. The smallest spectral interval ΔE which can be resolved is therefore

$$\Delta E = \frac{1}{\mathcal{D}} \frac{\Delta x}{\mathcal{F}}, \quad (1)$$

where Δx is the largest of either the source S image size on the detector for a particular monochromatic component or detector spatial resolution.

Nowadays, diffraction grating manufacturing technology has advanced to the extent that grating spectrographs are being successfully used with much shorter wavelengths, in particular in soft x-ray regime ($\lesssim 1 \text{ keV}$) [13] attaining a resolving power of $E/\Delta E \simeq 10^4$. Extension into the hard x-ray regime is, however, not trivial, because of the lack of hard x-ray optics elements with sufficiently large dispersion rate.

A hard x-ray equivalent of the diffraction grating is a Bragg diffracting crystal with diffracting atomic planes at an asymmetry angle $\eta \neq 0$ to the entrance crystal surface - Fig. 1(b) [5, 7, 8]. The AD rates in Bragg diffraction are typically small $\mathcal{D} \simeq 8 \mu\text{rad}/\text{meV}$ [6], being the main

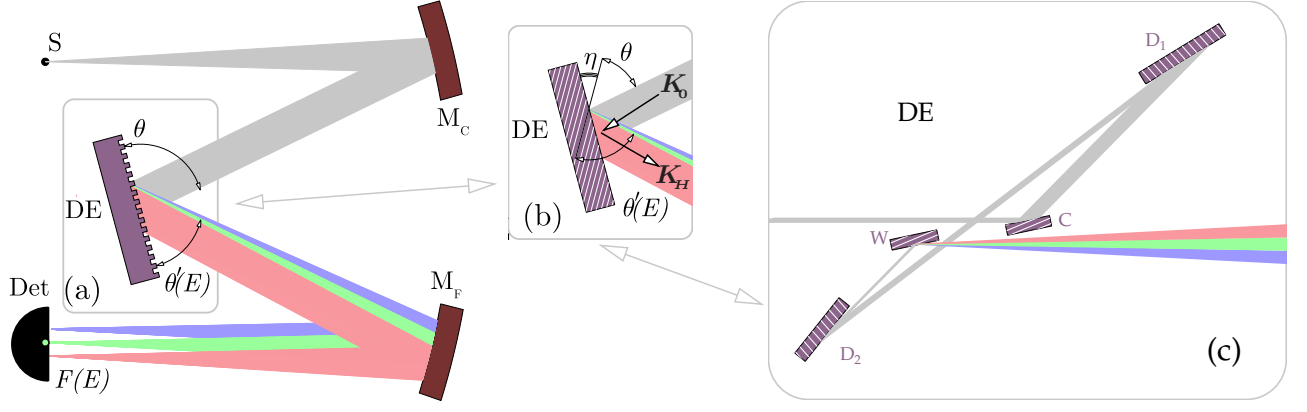


FIG. 1: Scheme of the Czerny-Turner type [10] spectrograph with a diffraction grating (a), or a crystal in asymmetric x-ray Bragg diffraction (b) as dispersing element - DE. Other components include radiation source S, collimating and focusing mirrors M_C and M_F , and position sensitive detector Det. (c) Multi-crystal multi-reflection CDFDW optics - is an example of a hard x-ray “diffraction grating” (DE element) with enhanced dispersion rate, suitable for hard x-ray spectrographs.

obstacle in realization of hard x-ray spectrographs [18]. The AD rate can be enhanced dramatically, by successive asymmetric Bragg reflections, as shown below.

Let \mathbf{K}_0 be the momentum of the incident x-ray photon, and \mathbf{K}_H of the photon reflected from a crystal in Bragg reflection with the diffraction vector \mathbf{H} . The vectors \mathbf{K}_0 and \mathbf{K}_H make angles $\theta + \eta$, and $\theta' - \eta$, respectively, with the crystal surface - Fig. 1(b). The asymmetry angle η is defined here to be positive in the geometry shown in Fig. 1(b), and negative in the geometry with reversed incident and reflected x-rays (not shown). Conservation of the tangential components $(\mathbf{K}_H)_t = (\mathbf{K}_0 + \mathbf{H})_t$ with respect to the entrance crystal surface, and the conservation of the photon energies $|\mathbf{K}_H|\hbar c = |\mathbf{K}_0|\hbar c = K\hbar c = E$ require that [14]:

$$\cos(\theta' - \eta) = \cos(\theta + \eta) + \frac{H}{K} \sin \eta. \quad (2)$$

Differentiating over E , using Bragg's law $2K \sin \theta = H$, and assuming $|\theta' - \theta| \ll 1$, we obtain

$$\frac{d\theta'}{dE} = -b \frac{d\theta}{dE} + \mathcal{D}, \quad \mathcal{D} = \frac{2 \sin \theta \sin \eta}{E \sin(\theta - \eta)} \quad (3)$$

Here $b = -\sin(\theta + \eta)/\sin(\theta - \eta)$ is the asymmetry ratio. If the incident beam is collimated, $d\theta/dE = 0$, then $d\theta'/dE = \mathcal{D}$, where \mathcal{D} (3) is the intrinsic AD rate in a Bragg reflection [5, 7]. If, however, the incident x-rays are dispersed, $d\theta/dE \neq 0$, then the dispersion rate $d\theta'/dE = \mathcal{D}_{\text{out}}$ becomes

$$\mathcal{D}_{\text{out}} = b\mathcal{D}_{\text{in}} + \mathcal{D}, \quad (4)$$

where $\mathcal{D}_{\text{in}} = -d\theta/dE$. The minus sign follows the convention that the counterclockwise sense of angular variations in θ and θ' is positive. Similarly, if the sense of deflection of the ray upon the Bragg reflection is clockwise, unlike that shown in Fig. 1(b), then \mathcal{D} in Eq. (3) has to be used with sign minus.

Equation (4) demonstrates that the AD rate \mathcal{D}_{in} can be indeed significantly enhanced by two successive asymmetric Bragg reflections, if its asymmetry ratio is large: $|b| \gg 1$. The enhancement can be even larger if several $(1, 2, \dots, n)$ successive reflections are used:

$$\mathcal{D}_{\cup_n} = b_n \mathcal{D}_{\cup_{n-1}} + \mathcal{D}_n = b_n (b_{n-1} \dots (b_3 (b_2 \mathcal{D}_1 + \mathcal{D}_2) + \mathcal{D}_3) \dots \mathcal{D}_{n-1}) + \mathcal{D}_n. \quad (5)$$

In the first experiment presented below, we demonstrate this effect on an example of a four-crystal angular dispersive CDFDW optics, with schematic shown in Fig. 1(c). In the second proof of principle experiment presented in this paper, we apply such optics as the “dispersion grating” of a prototype hard x-ray spectrograph to image a spectrum of the CDFDW with record high spectral resolution. The experiments were performed at 30ID beamline of the APS.

Details on the CDFDW optics used in this paper are provided in [9]. CDFDW is a modification of the CDW [5, 6] optics originally designed to achieve the very high monochromatization of x-rays. The first element - C (collimator) - is a Si asymmetrically cut crystal, with the 220 Bragg reflection, $\theta_C = 20.7^\circ$, $\eta_C = 19.0^\circ$, $b_C = -1/21.5$, accepting x-rays with photon energy $E = 9.1315$ keV in a wide angular range $\simeq 110 \mu\text{rad}$, and collimating it to a beam with a $|b_C|$ smaller divergence, and negligible $\mathcal{D}_C = 0.040 \mu\text{rad/meV}$. The next two Si crystals - D_1 and D_2 , are designed to produce maximal intrinsic Bragg dispersion rate \mathcal{D} (3), using the 008 reflection with $\theta_{D_i} \simeq 90^\circ$, $\eta_{C_i} = 88.0^\circ$, $b_{D_i} \simeq -1$ ($i = 1, 2$), and $\mathcal{D}_{D_1} = -\mathcal{D}_{D_2} = 6.27 \mu\text{rad/meV}$. Note, that the scheme in Fig. 1(c) is shown in a generic configuration with $\theta_{D_i} \neq 90^\circ$. The fourth crystal - W, is equivalent to the C-crystal, however applied in an inverse configuration with $\eta_W = -\eta_C$, $b_W = 1/b_C = -21.5$, and $\mathcal{D}_W = 0.86$. It is used to enhance the AD rate

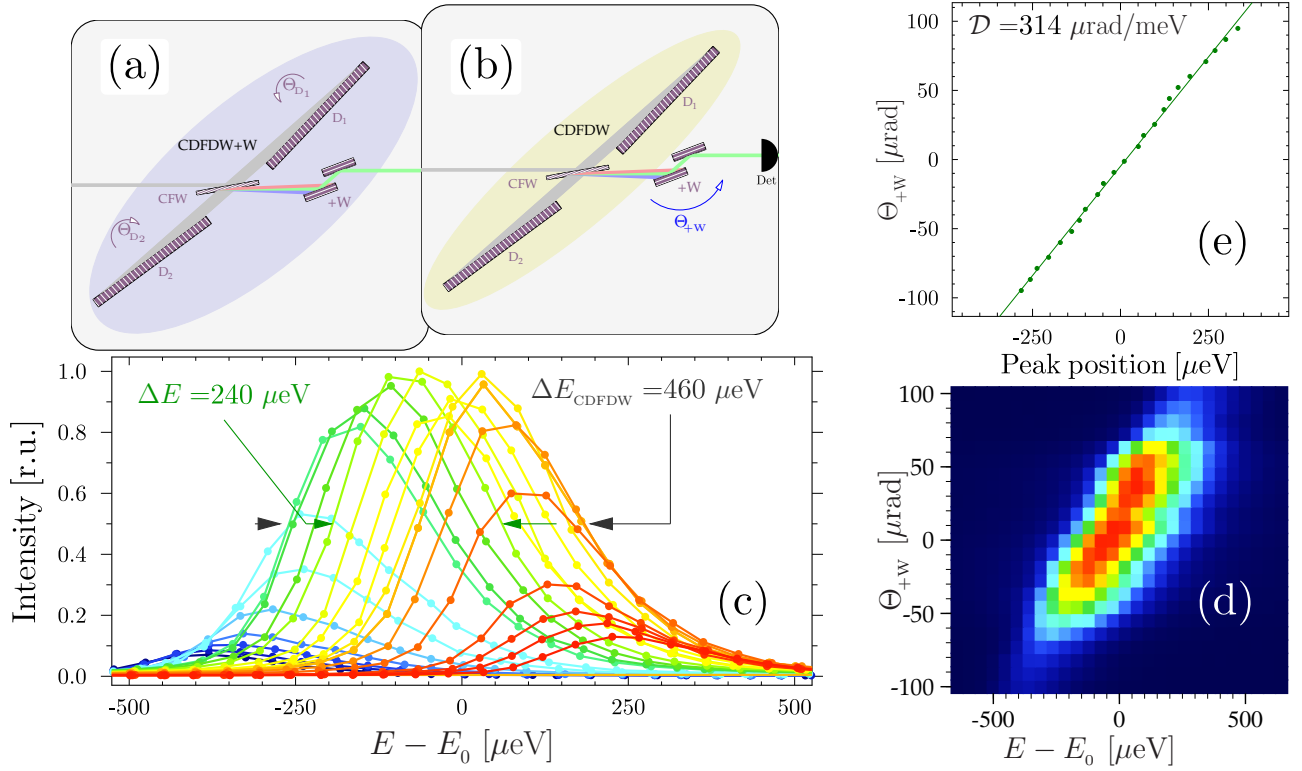


FIG. 2: Enhanced angular dispersion rate of the CDFDW optics. Schematic of the experiment showing the CDFDW+W monochromator (a) probing the angular dispersion rate of the CDFDW optics (b) with the +W channel-cut crystal as an angular analyzer. (c) Spectral dependences of x-ray transmission through the CDFDW optics for fixed angular positions Θ_{+W} of +W. (d) Same as (c) presented as a 2D plot. (e) Transmission peak position as a function of Θ_{+W} .

of the D-crystals. Indeed, applying Eq. (5) we estimate the cumulative dispersion rate of the optics: $\mathcal{D}_U \simeq b_w(\mathcal{D}_{D_2} - \mathcal{D}_{D_1}) + \mathcal{D}_w \simeq 2b_w\mathcal{D}_{D_1} \simeq -270$ μrad/meV, enhanced by a factor $2|b_w| \simeq 43$ compared to the dispersion rate achieved in a single Bragg reflection. The same enhancement factor was derived in [15] using DuMond diagram analysis.

Figure 2 shows a schematic of the first experiment and results of measurements of the AD rate of the CDFDW optics. A tunable monochromator with a $\simeq 170$ μeV bandwidth shown schematically in Fig. 2(a), and described in detail in the next paragraph, is used to measure transmission spectra through the CDFDW optics under study, presented in Fig. 2(b). An auxiliary element denoted as +W in Fig. 2(b), is used to extract from all x-ray photons emanating from the CDFDW optics a small part with $\simeq 20$ μrad divergence by the 220 symmetric Bragg reflection (angular acceptance 20 μrad) from a Si channel-cut crystal. For each angular position Θ_{+W} of the +W crystal, a spectrum of x-rays transmitted through the CDFDW optics and through the +W angular analyzer is measured, as shown in Fig. 2(c). Figure 2(d) presents a 2D plot of the spectra. The peak of the spectral distribution changes with the emission angle defined by Θ_{+W} . Figure 2(e) shows that the dependence is linear,

with the tangent $\mathcal{D}_{\text{CDFDW}} = 314$ μrad/meV representing the measured dispersion rate of the CDFDW optics. The number is even higher than the previously estimated one, which we attribute to the difference between the nominal and real asymmetry angles. The result confirms the theoretical prediction, expressed by Eqs. (4)-(5), that the angular dispersion rate can be substantially enhanced in multi-crystal arrangements.

A few details regarding the monochromator in Fig. 2(a) are in order: It is the same CDFDW optics, however, enhanced with the +W channel-cut that substantially decrease the CDFDW bandwidth.

The energy tuning of the CDFDW+W monochromator is performed by synchronous change of the angular orientation of the D-crystals, as indicated by Θ_{D_i} in Fig. 2(a), and explained in more detail in [9]. Each spectral dependence in Figure 2(c) has a width of $\Delta E \simeq 240$ μeV. This number represents the width of the convolution of the spectral distributions of the CDFDW+W monochromator - Fig. 2(a), and the analyzer - Fig. 2(b). Assuming they are equivalent, the spectral width of a single CDFDW+W optics is estimated as $\Delta E/\sqrt{2} \simeq 170$ μeV. An envelope of spectral dependences in Fig. 2(c) reveals a total width of $\Delta E_{\text{CDFDW}} \simeq 460$ μeV, and represents the spectral width of the CDFDW optics. A similar number

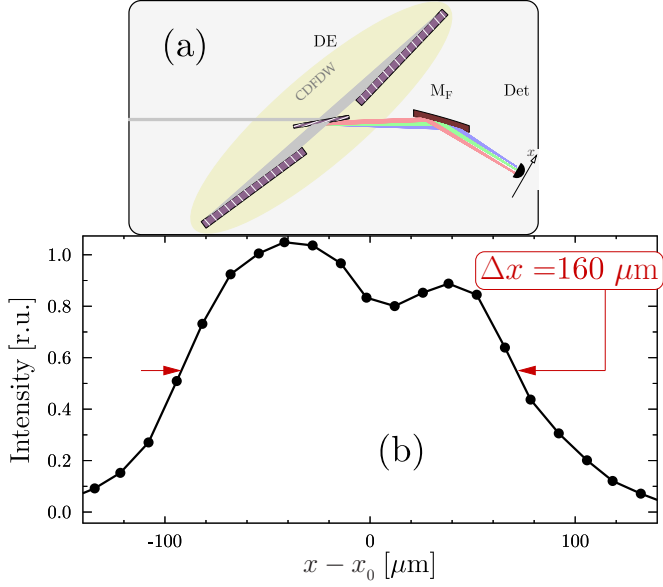


FIG. 3: Image of the CDFDW spectral function on the spatial x -scale (b) measured in the prototype spectrograph setup (a).

has been measured in [9].

In the second experiment, the CDFDW optics with the demonstrated above greatly enhanced dispersion rate is used as a “dispersion grating” of a prototype hard x-ray spectrograph. The enhanced dispersion rate enables imaging of the CDFDW spectrum with a record high spectral resolution. Figure 3(a) shows the proof of the principle spectrograph setup, in which the CDFDW optics is augmented with a focusing mirror M_F and a position sensitive detector placed at the mirror focal distance $\mathcal{F} = 1.38$ m. The polychromatic collimated beam, which in a complete spectrograph setup would be created by the collimating mirror M_C , as in Fig. 1(a), is mimicked here by the incident x-ray beam with a $\lesssim 15 \mu\text{rad}$ angular divergence and a bandwidth of $\simeq 0.6$ eV. This beam is focused by mirror M_F to produce a spot with a $\simeq 30 \mu\text{m}$ size. Figure 3(b) shows the spatial distribution of x-rays transmitted through the CDFDW optics and imaged on the detector with mirror M_F . It is $\simeq 160 \mu\text{m}$ broad, i.e., much broader than the $\simeq 30 \mu\text{m}$ image size of the incident beam, and has a double peak structure. We believe that this distribution presents the image of the spectrum of x-rays transmitted through the CDFDW optics, mapped on x using mirror M_F . It correspond to the envelope of spectral dependences shown in Fig. 2(c), however with a more pronounce minimum near $x = 0$, as no convolution with the monochromator spectral function is involved. The spatial width $\Delta x \simeq 160 \mu\text{m}$ corresponds to the spectral width, which we know should be $\simeq 450 \mu\text{eV}$. The results shown in Fig. 4(b), which were measured in a modified experimental scheme presented in Fig. 4(a), confirm this.

The experiential scheme in Fig. 4(a) is complemented by the +W channel-cut which, as we know from the results presented in Fig. 2, selects x-ray emanating in a certain direction from the CDFDW optics, and, as a result, within a reduced bandwidth, whose central photon energy is defined by the angle Θ_{+W} . Figure 4(b) shows the spatial distribution of x-rays measured at different Θ_{+W} values. The peak positions, plotted in Figure 4(d), change linearly with Θ_{+W} at a rate $\mathcal{D}_F = 1.13 \mu\text{m}/\mu\text{rad}$. Together with the results presented in Fig. 2(e) this proves that the spectral distribution of x-rays from the CDFDW optics is imaged by mirror M_F on the spatial scale, with a conversion factor $\mathcal{D}_F \mathcal{D}_{\text{CDFDW}} \simeq 355 \mu\text{m}/\text{meV}$. Using this number, we obtain that the total widths of the spatial distributions in Figs. 3(b) and 4(b) are $\Delta_{\text{CDFDW}} \simeq 450 \mu\text{eV}$, representing the spectral width of the CDFDW optics. The spatial widths of single lines vary from $32 \mu\text{m}$ (in green) to $50 \mu\text{m}$ (in yellow), corresponding to spectral widths $\simeq 90 \mu\text{eV}$ and $\simeq 140 \mu\text{eV}$ respectively. The resolution of the CDFDW spectrograph is at least $\simeq 90 \mu\text{eV}$, or better. The fact that this value changes across the CDFDW spectrum, as well as the fact that the CDFDW spectrum has a double-peak structure, imply that the CDFDW optics we have built is not yet perfect. This is consistent with the results of [9], where a somewhat broader line was measured as expected from theory. However, now using the CDFDW in the spectrograph setup, we can measure and analyze the CDFDW spectrum directly, without the need of another CDFDW optics as an analyzer. Using Eq. (1) with $\mathcal{F} = 1.38$ m, $\Delta x = 32 \mu\text{m}$, and the theoretically estimated $\mathcal{D}_U = 270 \mu\text{rad}/\text{meV}$, we obtain $\Delta E = 86 \mu\text{eV}$ in agreement with the measured energy resolution.

In conclusion, a principle is proposed and demonstrated how to enhance by more than an order of magnitude the angular dispersion rate of x-rays in Bragg diffraction, namely by successive asymmetric Bragg reflections. This effect opens an opportunity of realizing dispersing elements in the hard x-ray regime with an angular dispersion rate sufficiently large for x-ray spectrographs. The hard x-ray spectrograph principle is demonstrated with the multi-crystal multi-reflection CDFDW optics as dispersing element, by imaging an x-ray spectrum of 9.1315 keV photons in a $450 \mu\text{eV}$ window with a record small $90 \mu\text{eV}$ resolution, thus achieving spectral resolution power beyond 10^8 in hard x-ray regime. The main future effort should be directed not only to further improving the spectral resolution, but primarily into making the spectral window broader, to enhance the spectrographs’ throughput. Hard x-ray spectrographs can advance significantly research using high-resolution x-ray spectroscopies, in particular different branches of inelastic x-ray scattering, using synchrotrons and seeded XFELs [16].

We are grateful to L. Young for supporting this project at the APS, to S. Collins and G. Materlik at the DLS.

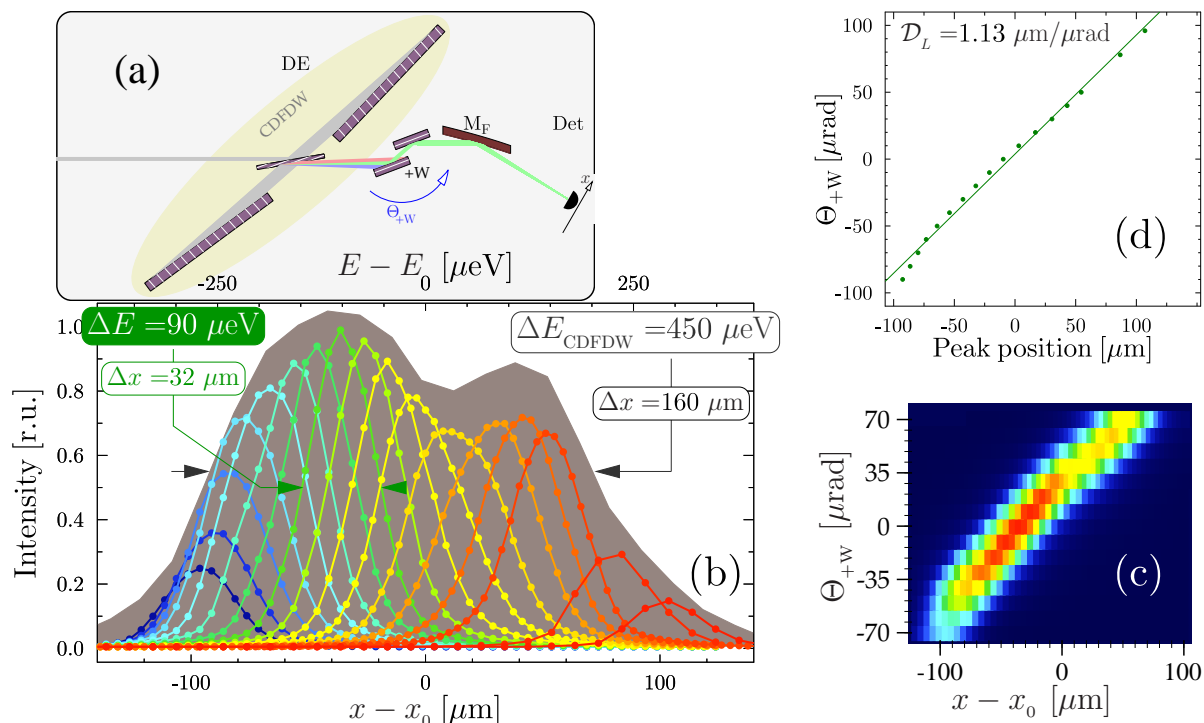


FIG. 4: Prototype hard x-ray spectrograph with a $\simeq 90\mu\text{eV}$ resolution using CDFDW optics as dispersing element (DE). (a) Schematic of the experiment. (b) Images of the CDFDW+W spectral function on the spatial x -scale for fixed angular positions Θ_{+W} of $+W$. (c) Same as (b) presented as a 2D plot. (d) Spatial peak position as a function of Θ_{+W} .

D. Shu, T. Roberts, K. Goetze, J. Kirchman, P. Jemian, M. Upton, and Y. Ding are acknowledged for technical support. R. Lindberg and X. Yang are acknowledged for reading the manuscript and valuable suggestions. Work was supported by the U.S. Department of Energy, Office of Science, Office of Basic Energy Sciences, under Contract No. DE-AC02-06CH11357.

* Electronic address: shvydko@aps.anl.gov

- [1] T. Matsushita and R. P. Phizackerley, Jpn. J. Appl. Phys. **20**, 2223 (1981).
- [2] S. Huotari, G. Vanko, F. Albergamo, C. Ponchut, H. Graafsma, C. Henriquet, R. Verbeni, and G. Monaco, J. Synchrotron Radiation **12**, 467 (2005).
- [3] M. Yabashi, J. B. Hastings, M. S. Zolotarev, H. Mimura, H. Yumoto, S. Matsuyama, K. Yamauchi, and T. Ishikawa, Phys. Rev. Lett. **97**, 084802 (2006).
- [4] D. Zhu, M. Cammarata, J. M. Feldkamp, D. M. Fritz, J. B. Hastings, S. Lee, H. T. Lemke, A. Robert, J. L. Turner, and Y. Feng, Appl. Phys. Lett. **101**, 034103 (2012).
- [5] Y. Shvyd'ko, *X-Ray Optics – High-Energy-Resolution Applications*, vol. 98 of *Optical Sciences* (Springer, Berlin Heidelberg New York, 2004).
- [6] Y. V. Shvyd'ko, M. Lerche, U. Kuetgens, H. D. Rüter, A. Alatas, and J. Zhao, Phys. Rev. Lett. **97**, 235502 (2006).
- [7] T. Matsushita and U. Kaminaga, Journal of Applied Crystallography **13**, 472 (1980).
- [8] S. Brauer, G. Stephenson, and M. Sutton, J. Synchrotron Radiation **2**, 163 (1995).
- [9] Y. Shvyd'ko, S. Stoupin, D. Shu, and R. Khachatryan, Phys. Rev. A **84** (2011).
- [10] M. Czerny and A. F. Turner, Z. f. Physik **61**, 792 (1930).
- [11] A. B. Shafer, L. R. Megill, and L. Droppelman, J. Opt. Soc. Am. **54**, 879 (1964).
- [12] K.-S. Lee, K. P. Thompson, and J. P. Rolland, Opt. Express **18**, 23378 (2010).
- [13] G. Ghiringhelli, A. Piazzalunga, C. Dallera, G. Trezzi, L. Braicovich, T. Schmitt, V. N. Strocov, R. Betemps, L. Patthey, X. Wang, et al., Rev. Sci. Instrum. **77**, 113108 (2006).
- [14] M. Kuriyama and W. J. Boettinger, Acta Cryst. **A32**, 511 (1976).
- [15] Y. Shvyd'ko, arXiv:1110.6662 (2011).
- [16] J. Amann, W. Berg, V. Blank, F.-J. Decker, Y. Ding, P. Emma, Y. Feng, J. Frisch, D. Fritz, J. Hastings, et al., Nature Photonics **6** (2012).
- [17] V. G. Kohn, A. I. Chumakov, and R. Ruffer, J. Synchrotron Radiation **16**, 635 (2009).
- [18] The use of asymmetrically cut crystal as dispersing element in combination with a focusing element was proposed for a “focusing monochromator” [17]. As was noticed in [17] such optics can be used as a monochromator, however, not as a spectral analyzer (or spectrograph), as a small angular size of the radiation source is required for its realization.